Arctic Haze : Current Trends and Knowledge Gaps

P.K. Quinn, NOAA PMEL, Seattle, WA, USA
G. Shaw, University of Alaska, Fairbanks, AK, USA
E. Andrews, University of Colorado, Boulder, CO, USA
E.G. Dutton, NOAA GMD, Boulder, CO, USA
T. Ruoho-Airola, Finnish Meteorological Institute, Helsinki, Finland
S.L. Gong, Air Quality Research Branch, Meteorological Service of Canada, Toronto, Ontario, Canada

For submission to *Tellus B*
June 20, 2006

Abstract. Trend analyses were performed on several indicators of Arctic Haze using data from sites located in the North American, Norwegian, Finnish, and Russian Arctic for the spring months of March and April. Concentrations of non seasalt (nss) $SO_4^=$ in the Canadian, Norwegian, and Finnish Arctic were found to have decreased by 30 to 70% from the early 1990s to present. The magnitude of the decrease depended on location. The trend in nss $SO_4^=$ at Barrow, Alaska from 1997 to present, is unclear. Measurements at Barrow of light scattering by aerosols show a decrease of about 50% between the early 1980s to the mid 1990s for both March and April. Restricting the analysis to the more recent period of 1997 to present indicates an increase in scattering of about 50% during March. Aerosol NO_3^- measured at Alert, Canada has increased by about 50% between the early 1990s to 2003. Nss K^+ and light absorption, indicators of forest fires, have a seasonal maximum during the winter and spring and minimum during the summer and fall at both Alert and Barrow. Based on these data, the impact of summertime forest fire emissions on low altitude surface sites within the Arctic is relatively small compared to winter/spring emissions. Key uncertainties about the impact of long range transport of pollution to the Arctic remain including the certainty of the recent detected trends; sources, transport, and trends of soot; and radiative effects due to complex interactions between aerosols, clouds, and radiation in the Arctic.

1. The Arctic Haze Phenomenon

It has been more than 50 years since observations of a strange haze, of unknown origin, were reported by pilots flying in the Canadian and Alaskan Arctic (Greenaway, 1950; Mitchell, 1956). Based on measurements at McCall Glacier in Alaska, Shaw and Wendler (1972) noted that the turbidity maximized in spring. First measurements of the vertical structure of the haze were made in an Alaskan "bush" airplane with a hand-held sunphotometer (Shaw, 1975). At that time the origin of the haze was uncertain and was attributed to ice crystals seeded by open leads or blowing dust from riverbeds. It was only through "chemical fingerprinting" of the haze that its anthropogenic source was revealed (Ottar et al., 1986; Rahn et al., 1977, Rahn and McCaffrey, 1979; Rahn 1989). By the late 1970's the anthropogenic origin was clear but surprising since it was widely believed that aerosol was generally not transported more than a few hundreds of km from its source regions. Experts from Europe and America convened at the first Arctic Air Chemistry Symposium at Lillestrom, Norway in 1978 and an informal measurement network was agreed upon. Spatial gradients soon showed the direction of flow and the surprisingly large extent of this anthropogenic cloud of pollution. A combination of intensive field programs and long term measurements extending over the past thirty years confirmed the early conclusions that the haze is anthropogenic in origin due to emissions from Europe and the former Soviet Union that are transported to and trapped in the Arctic air mass during the winter and early spring.

The haze is composed of a varying mixture of sulfate and particulate organic matter (POM) and, to a lesser extent, ammonium, nitrate, dust, and black carbon (e.g., Li and Barrie, 1993; Quinn et al., 2002). It also is rich in distinct heavy metals which has allowed for the identification of particular industrial sources (eg. Shaw, 1983; Polissar et al., 1998; 2001). Particles within the haze are well-aged with a mass median diameter of about 0.2 microns or less (e.g., Heintzenberg, 1980; Hoff et al., 1983; Pacyna et al., 1984; Shaw, 1984; Leaitch et al., 1989; Trivett et al., 1989; Clarke, 1989; Hillamo et al., 1993). This particle size range is very efficient at scattering visible solar radiation since the peak in the particle surface-area size distribution is near the maximum efficiency for Mie scattering (Waggoner and Weiss, 1980; Shaw, 1987). The haze also is weakly absorbing due to the presence of black carbon (e.g., Hansen and Rosen, 1984; Noone and Clarke, 1988; Kahl and Hansen, 1989; Hopper et al., 1994). The result of the strong scattering and weaker absorption

is a noticeable reduction in visibility to a few kilometers or less. The "weak" absorption may have large climatic influences when the dark colored haze spreads out over the highly reflecting snow and ice pack of the Arctic. The highly reflecting surface enhances aerosol-radiative interactions due to multiple scattering between the surface and the haze (e.g., Shaw and Stamnes, 1980).

Several seasonally-dependent mechanisms contribute to the formation of Arctic Haze. Strong surface-based temperature inversions form in the polar night causing the atmosphere to stabilize. This cold and stable atmosphere inhibits turbulent transfer between atmospheric layers as well as the formation of cloud systems and precipitation, the major removal pathway for particulates from the atmosphere (Barrie et al., 1981; Shaw, 1981;1995; Heintzenberg and Larssen, 1983). In addition, meridional transport from the midlatitudes to the Arctic intensifies during the winter and spring (Iversen and Joranger, 1985). The combination of these factors results in the transport of precursor gases and particulates to the Arctic and the trapping of the pollutant haze for up to 15 to 30 days (Shaw, 1981;1995).

Aircraft and lidar measurements throughout the 1980s and 1990s revealed that the haze occurs primarily in the lowest five kilometers of the atmosphere and peaks in the lowest two kilometers (Leaitch et al., 1984; Barrie, 1996; Hoff, 1988; Pacyna and Ottar, 1988). Throughout the haze season, the pollution layers are highly inhomogeneous both vertically (tens of meters to 1 km thick) and spatially (20 to 200 km in horizontal extent) (Radke et al., 1984; Brock et al. 1989).

Recent aircraft measurements of sulfate aerosol using a high time resolution technique revealed detailed information about the evolution of the vertical structure of the haze between February and May (Scheuer et al., 2003). During early February, significant enhancements in sulfate aerosol are confined near the surface (< 2 km) as long range transport from northern Eurasia occurs along low level, sinking isentropes (Klonecki et al., 2003). As the haze season progresses, enhanced sulfate occurs at higher altitudes (up to at least 8 km). Since vertical mixing is prohibited by the persistent low-level inversion (Kahl, 1990), the higher altitude haze layers are thought to be due to transport into the Arctic along vertically higher isentropes tracing back to increasingly warmer source regions in northern Eurasia. During early April, sulfate layers below 3 km begin to dissipate due to the beginning of solar heating and resulting mixing near the surface. However, more stable isentropic transport continues at higher altitudes. By the end of May, both the lower and higher altitude sulfate

enhancements are significantly decreased due to the continued break-up of the inversion and return of wet deposition.

Recent studies also have provided evidence for an influence of natural climate variability on interannual changes in levels of Arctic haze. Modeling the dispersion of anthropogenic emissions from northern hemisphere continents, Eckhardt et al. (2003) found that the North Atlantic Oscillation (NAO) influences pollution transport into the Arctic during the winter-spring haze season. During positive phases of the NAO, surface concentrations of modeled tracers in the Arctic winter were found to be elevated by about 70% relative to negative phases. This difference was mainly due to a change in pathways of European pollution and, to a lesser extent, North American pollution to the Arctic both of which are enhanced during positive NAO phases. In addition, during positive NAO phases, significant positive correlations between the NAO and measured CO concentrations were found at three Arctic stations (Spitsbergen, Barrow, and Alert) confirming enhanced poleward transport of pollution from Europe, Asia, and North America. Similar but weaker correlations between the NAO and measured CO were found for spring. Low correlations were found during summer and fall.

During transport from the source regions to the Arctic, the pollutant-containing air masses have a high probability of reaching saturation and nucleating and precipitating clouds. It is not understood how so much material gets through a strongly scavenging system (Bowling and Shaw, 1992).

Arctic Haze has been the subject of much study because of its potential to change the short and longwave radiation balance of the Arctic, affect visibility, and provide a source of contaminants to Arctic ecosystems. The near surface concentration of aerosols at most places in the Arctic are about an order of magnitude lower than those found at more polluted and industrialized locations. At the same time, however, the affected areas are much larger in size and the affected ecosystems in the high Arctic are thought to be quite sensitive to gaseous and aerosol contamination.

It is not known what fraction of the Arctic Haze contaminants leave the Arctic and what fraction is deposited within the Arctic on land and sea surfaces. As the polar night ends, some of the pollution that has accumulated is released to the mid-latitudes (Penkett et al., 1993; Heintzenberg et al., 2003). It is known that haze contaminants (e.g., acidic sulfate and organics) end up in Arctic ecosystems (Meijer et al., 2003; Wania, 2003) but the timing and mechanism of the scavenging from the atmosphere is

not well understood. Measurements from a 5 m snow pit and 75 m ice core in Greenland indicated that there is a maximum in sulfate and black carbon deposition to the surface during the Arctic haze season although there can be significant deposits throughout the year (Masclet et al., 2000). Similarly, sulfate concentrations as well as concentrations of other Arctic haze tracers (Pb, Cd, and As) in snow at sixteen sites across northwest Alaska were found to be highest in the later winter snow pack (Douglas and Sturm, 2004). The aerosols are removed from the atmosphere either through dry deposition or wet deposition with the mechanism of the latter most likely involving nucleation followed by precipitation in the form of ice crystals (Masclet et al., 2000). Since the timing of the buildup of the haze and the snow pack is similar and haze concentrations decline before the snow has fully melted, it is likely that haze contaminants first enter the ecosystem by being deposited in the snow (Douglas and Sturm, 2004). Contaminants deposited in the snow then end up in the tundra and rivers as the snow melts. The network of snow measurements across northwest Alaska showed spatially homogeneous concentrations in sulfate and trace elements suggesting little variability in atmospheric concentration or scavenging efficiency within the confines of the sampled region. By contrast, the acidity of the snow was much patchier indicating that competing acidifying and buffering sources determine the local pH. For example, pH was consistently higher in the Brooks Range than elsewhere due to mechanical weathering of carbonate rocks.

2. Trends in Arctic Haze

2.1. Chemical composition.

Arctic Haze is marked by a dramatic increase in concentrations of several key particulate pollutants during winter and early spring. The seasonal trend in the haze has been detected at several monitoring sites in the Arctic including Alert (82.46°N) in the Canadian Arctic, Station Nord in Greenland (81.4°N), Zeppelin (79°N) on the island of Svalbard, Barrow in Alaska (71.3°N), Karasjok (69.5°N) and Svanvik (69.45°N) in northern Norway, Oulanka (66.3°N) in northern Finland, and Janiskoski (69°N) in western Russia. (Figure 1). A time series of particulate sulfate is shown for these eight monitoring sites in Figure 2. Each site has a similar winter/early spring increase in sulfate with maximum concentrations reaching up to about 1 μg S m^{-3}. Summertime monthly average concentrations are less than 0.03 μg S m^{-3}. Nss (non-seasalt) sulfate makes up about 30% of the submicron mass during the haze season

(Barrie et al., 1981; Quinn et al., 2000; 2002). Figure 3 shows the time series of particulate nitrate at Alert and Barrow, two sites which have a clear seasonal pattern for this chemical species. Maximum concentrations are near 0.04 μg N m^{-3}. Other species also indicative of continental sources (nss K^{+} for biomass burning and Mg^{+2} and Ca^{+2} for dust) have maximum concentrations in winter and spring indicating long range transport to the Arctic (Figure 4) (Quinn et al., 2002).

Natural aerosol chemical components display seasonal cycles quite different from anthropogenic components. Submicrometer sea salt concentrations are highest at Alert and Barrow from November through February (Quinn et al., 2002). The winter maximum has been attributed to seasonally high winds in high-latitude source regions of the Pacific and Atlantic Oceans and long range transport to the Arctic (Sturges and Barrie, 1988, Sirois and Barrie, 1999). Supermicron sea salt aerosol is at a maximum during the summer months at Barrow when the ice pack extent is at a minimum (Quinn et al., 2002). Atmospheric methanesulfonic acid or MSA^{-} is derived solely from the oxidation of biogenically produced dimethylsulfide (DMS). Concentrations of MSA^{-} begin to increase in late June as the ice recedes and phytoplankton productivity in surface waters begins (Figure 5). In addition, DMS that has been trapped under the ice is released (Ferek et al., 1995).

Two years of measurements at a site in northern Finland revealed that particulate organic matter (POM) made up, on average, 22% of the total fine aerosol mass (range of 3 to 69%) (Ricard et al., 2002). Correlation of POM with nss sulfate was low indicating that POM is of a different origin than nss sulfate. Since POM displayed a seasonal cycle with maximum concentrations in the summer, it most likely is a result of biogenic emissions and/or enhanced oxidation processes. There is a small increase in organic acids as early as February/March which may be an indication of photooxidation at polar sunrise as was pointed out for Alert by Kawamura et al. (1996).

The longest record of sulfate concentrations in the Arctic (1980 to present at Alert, Canada) revealed no change in sulfate concentrations during the 1980s (Sirois and Barrie, 1999). This lack of a trend was attributed to little change in emissions in the former Soviet Union between 1985 and 1990. Beginning in 1991, sulfate and other measured anthropogenic constituents (Pb, Zn, Cu, excess V and Mn, and ammonium)

began to decline suggesting that the reduction of industry in the early years of the new Eurasian republics led to lower levels of pollutants reaching the Arctic.

A combined modeling and measurement analysis of sulfate concentrations at Station Nord in northern Greenland indicated a decreasing trend throughout the 1990s (Heidam et al., 2004). The analysis was able to account for scatter in measured concentrations due to changing meteorology. With the meteorological variability removed, they were able to attribute the decrease in concentration to a reduction in emissions. The model that was used estimates that more than 70% of the sulfur measured at Station Nord is emitted from the area making up the former Soviet Union so that the trend analysis indicates that emissions from that region decreased significantly during the 1990s. This result is supported by the 50% decrease in Russian sulfur emissions reported to EMEP during the 1990s (Vestreng, 2003). It is not clear from this analysis how reductions from Western Europe and North America influenced the sulfate concentrations at Station Nord.

As pointed out by MacDonald et al. (2005), the detection of recent trends in the Arctic is difficult due to the combination of short or incomplete data records at some sites and interference from natural variations on seasonal, annual, and decadal time scales. To remove seasonal variability from the trend analyses, we focus here on average monthly concentrations for March and April which are two of the months during with Arctic Haze is most pronounced (Bodhaine and Dutton, 1993). The existence of a monotonic increasing or decreasing trend in the time series was tested with the nonparametric Mann-Kendall test at significance levels $p<0.001$, $p<0.01$, and $p<0.1$ as a two-tailed test (Gilbert, 1987). The estimate for the slope of a linear trend was calculated with the nonparametric Sen's method (Sen, 1968). The Mann-Kendall test is suitable for cases where the trend may be assumed to be monotonic such that no seasonal or other cycle is present in the data. In the Mann-Kendall test, missing data values are allowed and the data need not conform to any particular distribution. The Sen's slope is the median of the slopes calculated from all pairs of values in the data series. The Sen's method is not greatly affected by data outliers and it can be used when data are missing (Salmi et al., 2002). Here, trends are only reported for a significance level of < 0.1, i.e., when the probability of no trend is 10% or less.

Average monthly concentrations of sulfate for March and April are shown in Figure 6 along with the Sen's slope estimates, the slope is given only for cases where the Mann-Kendall test yields a trend at a significance level of <0.1. The significance

of the trend, slope estimate, and percent change over the measurement period are given in Table 1. For sites with a significant trend (based on the Mann-Kendall test), sulfate concentrations decreased by 30 to 60% between 1990 and present. The decreasing trend in sulfate at Alert detected through the 1990s has continued into the present century. In addition, sulfate has decreased significantly at Zeppelin, Karasjok, and Oulanka.

Identical data are shown for nitrate in Figure 7 and Table 2. In contrast to sulfate, nitrate increased during April at Alert for the long-term period of 1981 to 2003 and during March for the shorter term more recent period of 1990 to 2003. Between 1990 and 2003, nitrate concentrations increased by about 50%.

2.2. Optical properties

The seasonality and trends of Arctic Haze are clearly seen in time series data of light absorption and scattering by aerosols measured at the surface (Figure 8) (Bodhaine, 1989; Delene and Ogren, 2002) and in total column aerosol optical depth (Dutton et al., 1984; Herber et al., 2002). Bodhaine and Dutton (1993) reported that both aerosol scattering and optical depth measurements at Barrow showed a maximum in 1982 followed by a factor of two decrease between 1982 and 1992. The decrease was only apparent during March and April corresponding to the time of year when Arctic Haze is most pronounced. The cause of the decrease is uncertain and most likely is due to a combination of factors. Bodhaine and Dutton (1993) hypothesized that the decrease in the haze was most likely due to a combination of a reduction in the output of pollution aerosol by Europe and the former Soviet Union and stricter pollution controls in Western Europe. The decreases in aerosol scattering and optical depth at Barrow during this ten year period are not equal to the known reductions of sulfate emissions, however, indicating that other factors such as changes in transport could have played a role (Jaffe et al., 1995). The NAO has been in a mostly positive phase since the 1970s. Since a positive phase implies enhanced transport of pollutants to the Arctic (Hurrell and van Loon, 1997), the NAO does not appear to have invoked the changes in transport responsible for the decreasing trend.

An update of the monthly averaged light scattering data analysis originally performed by Bodhaine and Dutton (1993) is shown in Figures 9 and 10 with data extending through 2006. Significance of the detected trends is given in Table 3 along with slope estimates and percent change in scattering for periods with linear trends. For March, there is a significant decreasing (but not linear) trend in scattering over the

entire measurement period of 1977 to 2006. Breaking the period into two smaller intervals reveals a decreasing linear trend from 1982 to 1996 which reverses to yield an increasing linear from 1997 to 2006. The increasing trend for March is significant at the 0.05 level indicating that there is a probability of 95% that the trend exists.

A similar analysis for light absorption at Barrow indicates an overall significant decrease between 1988 and 2006 for March. Trends between 1997 and 2006 are unclear (Figures 9 and 10; Table 3). Sharma et al. (2006) report an increasing trend in absorption for the winter months (defined as January through April) at Barrow between 2000 and 2003.

Black carbon concentrations derived from measured light absorption (often called equivalent black carbon) at Alert show a decreasing trend for both March and April over the measurement period of 1990 through 2001 (Figures 9 and 10; Table 3). Sharma et al. (2004) reported a decrease in (equivalent) black carbon (the main light absorber in the Arctic atmosphere) of 56% for the winter/spring season from 1989 to 2002 at Alert. However, Sharma et al. (2006) report an increase during winter (January to April) beginning in 2000.

A recent study using a general circulation model suggested that one of the major sources of Arctic soot today is southern Asia (Koch and Hansen, 2004) due to increasing emissions from industrial and biofuel combustion. This conclusion has been refuted by Stohl (2006), however, based on the long passage from pollution sources in south and east Asia to the Arctic relative to more rapid transport from Europe and northern Asia. Using a particle dispersion model, it was found that, for a transport time of 5 days, the south Asia black carbon contribution is about 1 to 2 % of the European source contribution near the surface and 3 to 5 % for the total column.

Results reported in Stohl (2006) identify boreal and temperate forest fires, especially Siberian fires, as a significant source of black carbon during the summer. It is suggested that in intense fire years, boreal forest fires may be the dominant source of black carbon for the Arctic. As measurements at Alert and Barrow show, there is a strong seasonal cycle in nss K^+ with minimum values in the summer and maximum values in the winter (Figure 4). Based on these data, the impact of summertime forest fire emissions on low altitude surface sites within the Arctic is relatively small compared to winter emissions. There is evidence, however, of pyrocumulonimbus injection of smoke from boreal forest fires to the upper atmosphere (Fromm et al., 2005). In addition, biomass burning signatures have been observed in the snow at the

high altitude (3200 m) site of Summit, Greenland (Dibb et al., 1996). The fraction of this material that is deposited to lower elevations throughout the Arctic is unknown. More measurements coupled with modeling studies are required to identify sources of black carbon to the Arctic and to assess trends in black carbon and light absorption by aerosols.

An extension of the Barrow aerosol optical depth data through 2002 shows a continued decrease through the mid 1990s (Figure 11). Monthly averaged values of AOD anomalies (relative to a base of non-volcanic years) for March show a continued decline through 2002. However, the AOD anomalies for April indicate an increase between 1998 and 2001 where the currently available data record ends. In contrast to the Barrow trend through the 1990s, Herber et al. (2002) report a slightly increasing trend in AOD (1% per year) at Koldewey station in Ny-Alesund, Spitzbergen between 1991 and 1999.

3. Effects of Aerosol on the Climate System in the Arctic

3.1. Direct Effect

The direct effect of aerosols on the radiation balance in the Arctic is due to the absorption and scattering of radiation by the aerosol. The Arctic is thought to be particularly sensitive to changes in radiative fluxes imposed by aerosols because of the small amount of solar energy normally absorbed in the polar regions (Valero et al., 1989). Arctic Haze is present as a layer of light absorbing material over a highly reflective ice/snow surface. Shaw and Stamnes (1980) first realized that the absorbing nature of Arctic haze would have a significant impact on the energy balance of the Arctic. Several early calculations using 1-D radiative transfer models estimated that the diurnally averaged atmospheric warming due to the layer ranged between 2 and 20 W/m2 with a corresponding depletion of the solar flux at the surface of 0.2 to 6 W/m2 (Leighton, 1983; Porch and MacCracken, 1982; Blanchet and List, 1987; Emery et al., 1992; Shaw et al., 1993). These estimates agreed with direct measurements from wideband sun photometers (Mendonca et al., 1981). Heating rates of about 0.1 to 0.2 K d^{-1} were measured by Valero et al. (1989) during AGASP (Arctic Gas and Aerosol Sampling Program) II and by Treffeisen et al. (2004) during the ASTAR 2000 campaign in Svalbard. The AASE (Airborne Arctic Stratospheric Expedition) II flights in winter of 1992 revealed soot contaminated Arctic aerosols at altitudes of 1.5 km. Pueschel and Kinne (1995) calculated that this layer of aerosols could heat the earth-atmosphere system above surfaces of high solar albedo (ice/snow) even for

single scattering albedos as high as 0.98. Hence, a modest amount of black carbon in the haze layers can result in a measurable contribution to diabatic heating.

MacCracken et al. (1986) estimated that the cooling of the surface due to absorption of solar radiation by the haze layers would be compensated by infrared emission from the atmosphere to the surface. The infrared emission is expected to dominate during the polar night when longwave radiation controls the energy budget of the Arctic. If the haze particles deliquesce thereby taking up water and growing to cloud droplet or ice crystal size, their longwave impact will be enhanced. Measurements made on Svalbard when the sun was below the horizon indicate that Arctic haze can have a measurable direct thermal radiative forcing altering the flux of downward longwave radiation by up to +3 to +4.7 W/m2 and the outgoing longwave radiation by -0.23 to +1.17 W/m2 (Ritter et al., 2005).

The vertical distribution of the absorbing haze layers does not affect the radiation budget at the top and bottom of the atmosphere (Cess, 1983) but may impact atmospheric circulation and climate feedback processes.

3.2. Indirect Effects.

The indirect effect of aerosols on irradiances in the Arctic results from the impact aerosol particles have on the microphysical properties of clouds. Enhanced aerosol particle concentrations increase solar cloud albedo by increasing the number concentration and decreasing the average size of cloud droplets provided the liquid water content in the clouds remains constant (Twomey, 1977). An increase in the number of pollution aerosol particles that act as cloud condensation nuclei (CCN) will affect Arctic stratus and stratocumulus by increasing the cloud droplet number concentration which results in more radiation being reflected back to space (Albrecht, 1989; Twomey, 1991). The relatively low aerosol number concentrations in the Arctic results in a large percentage of particles activating during cloud formation. Hence, changes in aerosol properties are likely to have a significant impact on microphysical and optical cloud properties. As the cloud droplet number concentration increases, cloud droplet size decreases which reduces drizzle formation and increases cloud coverage and lifetime potentially leading to less deposition of haze contaminants within the Arctic (Hobbs and Rangno, 1998).

Garrett et al. (2004) showed that low-level Arctic clouds are highly sensitive to particles that undergo long range transport during the winter and early spring. The sensitivity was detected as higher cloud droplet number concentrations and smaller

cloud droplet effective radii compared to summertime clouds exposed to particles nucleated in the Arctic from local biogenic sources. In addition, Arctic stratus appears to be more sensitive to pollutant particles than clouds outside of the Arctic. The most significant effect of the change in cloud properties due to Arctic Haze may be on cloud emissivity. A decrease in droplet effective radius in these optically thin clouds will increase the infrared optical depth and thus the infrared emissivity (Curry and Herman, 1985; Garrett et al., 2002). The result is expected to be an increase in downwelling infrared irradiances from the cloud and an increase in the rate of spring-time snow pack melting (Zhang et al., 1996).

According to observations during the SHEBA experiment, supercooled cloud droplets are common in the Arctic even at temperatures of -20°C or lower (Curry, 1995). The sulfate-containing pollution aerosol within Arctic Haze also is thought to impact ice nucleation. Models estimate that aerosols containing sulfuric acid produce fewer ice nuclei than nearly insoluble aerosols (Blanchet and Girard, 1995). Measurements corroborate this finding. Borys (1989) reported that Arctic haze aerosol had lower ice nuclei (IN) concentrations, a lower IN to total aerosol fraction, and slower ice nucleation rates than aerosol from the remote unpolluted troposphere. The reduction in ice nuclei leads to a decrease in the ice crystal number concentration and an increase in the mean size of ice crystals (Girard et al., 2005). As a result, the sedimentation and precipitation rates of ice crystals increase leading to an increase in the lower troposphere dehydration rate and a decrease in the downwelling infrared irradiances from the cloud. Using a 1-D simulation and observations from Alert, Girard et al. (2005) found that a cloud radiative forcing of -9 W/m2 may occur locally as a result of the enhanced dehydration rate produced by sulfate aerosol. The mechanism by which IN concentrations are decreased in the presence of sulfuric acid aerosol has yet to be explained and warrants further research. If this mechanism applies to much of the Arctic, it could explain the cooling tendency in the eastern high Arctic during winter.

Because of the combination of the static stability of the Arctic atmosphere, the persistence of low level clouds, and the relatively long lifetime of aerosols during the haze season, the impact of aerosols on cloud microphysical and optical properties may be larger in the Arctic than elsewhere on earth (Curry, 1995, Garrett et al., 2004). The winter/spring occurrence of Arctic haze events enables the study of anthropogenic influences against a very clean atmospheric background. In other regions of the globe,

a reliable distinction between natural and anthropogenic effects is more difficult. In this sense, the Arctic is a natural laboratory to study the anthropogenic portion of the aerosol-cloud-radiation interactions.

3.3. Surface Albedo

Surface albedo affects the magnitude and sign of climate forcing by aerosols. Absorbing soot deposited to the surface via wet and dry deposition impacts the surface radiation budget by enhancing absorption of solar radiation at the ground and reducing the surface albedo (Warren and Wiscombe, 1980). Clarke and Noone (1985) found a 1 to 3 % reduction in snow albedo due to deposited BC with another factor of 3 reduction as the snow ages and BC becomes more concentrated. Hansen and Nazarenko (2004) have estimated that soot contamination of snow in the Arctic and the corresponding decrease in surface albedo yields a positive hemispheric radiative forcing of +0.3 W m^{-2}. The resulting warming may lead to the melting of ice and may be contributing to earlier snowmelts on tundra in Siberia, Alaska, Canada, and Scandanavia (Foster et al., 1992; Stone et al., 2002a).

Clearly, the radiative impacts of pollutant aerosols in the Arctic are complex. Complex feedbacks between aerosols, clouds, radiation, sea ice, and vertical and horizontal transport processes complicate the impact as do potentially competing effects of direct and indirect forcing. As a result, the magnitude and sign of the forcing for the Arctic are not yet well understood.

3.4. Calculated Direct Radiative Forcing of Arctic Haze

The direct radiative forcing of Arctic Haze was calculated for a representative case during the haze maximum (mid-April) and for the latitude of Barrow. A two-stream radiative transfer model was used over the wavelength range of 300 to 1100 nm in 100 nm wide intervals. Multiple reflections between the surface and the haze layer were taken into account using calculations similar to those of Coakley and Chylek (1975) and Twomey (1977). The model requires knowledge of the albedo of the underlying surface (A), the aerosol optical depth (τ), single scattering albedo (ω), and the fraction of upward scattered radiation (β). Values employed for each of these parameters in the calculations and the basis for their use are listed in Table 4. In mid April, in the Alaskan sector of the Arctic, cloudiness is at its annual minimum and the region of Barrow is frequently under the influence of anticyclonic flow. Hence, cloudiness is assumed to be zero in the calculations. Direct radiative forcing in the

thermal infrared by Arctic Haze is not considered here although recent measurements indicate it may be non-negligible (Ritter et al., 2005).

Table 4 shows the results for conditions typical of the latitude of Barrow during spring haze maxima. The slightly absorbing haze results in a net heating of the earth-atmosphere system estimated to be 2.5 W m^{-2} averaged over a day. The absorbing and scattering haze above the highly reflecting snow surface results in a slightly negative net radiation balance or cooling at the surface of 0.93 W m^{-2}. The difference, 1.6 W m^{-2}, is absorbed in the haze layer itself. Calculations for a lower surface albedo of 0.2, which would be representative of the tundra after snow melt in late spring, results in a cooling due to the same amount of haze of 4 W m^{-2}. However, normally by the time snow melt in mid-May, Arctic Haze has disappeared.

The heating of the atmosphere by the haze may be calculated from

$$dT/dt = g*\Delta F/Cp*\Delta P \qquad (1)$$

where dT/dt is the heating in K s^{-1} (but expressed here in K d^{-1}), g is the acceleration of gravity, Cp is the specific heat of air (1006 J K^{-1} kg^{-1}) and P is pressure. Assuming the haze to be in a region 1 km thick (ΔP = 100 hPa), the heating rate is calculated to be 0.25K d^{-1}. The heating is due to multiple reflections, each absorbing some radiation, brought about by the underlying highly reflective surface.

The calculated radiative forcing values shown in Table 4 are lower but of the same sign as previous calculations. Shaw and Stamnes (1980) estimated a heating at TOA of 19 W m^{-2} and cooling at the surface of 5.3 W m^{-2}. The factor of six disagreement with the current calculations is due to a much lower value of single scattering albedo (0.6) used in the earlier calculations. The value of 0.6 was based on measurements of light reflected from filters exposed to aerosols and, although, there are systematic errors known to be associated with this type of determination, it may also be that the haze was sootier two decades ago. Less efficient flue gas cleanup employed in eastern Europe and the former Soviet Union may have led to a stronger and "blacker" Arctic Haze such that the radiative forcings were several times those calculated using more recent values of the haze optical properties.

Net radiative forcing is very sensitive to even relatively small perturbations in the amount of soot present in the transported haze. At the top of the atmosphere, a +3.1% change in radiative forcing results from a 1% increase in single scattering albedo. Hence, a slightly sootier haze could cause substantial heating of the Arctic regions in spring. Doubling the aerosol optical depth of the haze would increase the radiative

forcing at the top of the atmosphere by a factor of 1.8 while increasing the cooling at the surface by a factor of 1.7.

The calculations described here indicate that the presence of Arctic Haze over a representative location in the Arctic during the time of maximum haze results in an estimated 2 to 3 W m^{-2} of additional heating to the atmosphere and a smaller, approximately 1 W m^{-2} of cooling at the surface. This amount of heating is significant when compared to the estimated forcing due to the increase in carbon dioxide since the industrial revolution (4.5 W m^{-2}). It may be even more significant when recognizing that models indicate that there is a factor of 2 to 4 polar amplification of temperature change introduced at high latitudes by radiative forcing.

4. Summary

Based on measurements of sulfate aerosol, a main constituent of Arctic Haze, and light scattering and extinction, the amount of the haze reaching the Arctic was either relatively constant or decreasing between the 1980s and early 1990s (Sirois and Barrie, 1999; Bodhaine and Dutton, 1993; Heidam et al. 2004). The updated trends in light scattering presented here show a continued decrease through the late 1990s with an increase in the first years of the 21st century at Barrow, Alaska. There also is evidence, although not as strong, of an increasing trend in black carbon during this same period at Alert, Canada. Sulfate appears to have continued decreasing into the 21st century based on measurements at Alert in the Canadian Arctic, Zeppelin on the island of Svalbard, Karasjok in northern Norway, and Oulanka in northern Finland. On the other hand, nitrate appears to be increasing at Alert with an unclear trend at Barrow. Continued measurements coupled with chemical transport models are required to better define emerging trends and to assess their causes.

Arctic Haze is generally understood to consist of antropogenically-generated material, and has often been attributed to sources in central Eurasia (Shaw, 1983). There are examples, however, of Asian dust entering the Alaskan sector of the Arctic from as long ago as the mid 1970s (e.g., Rahn et al., 1981). Recent modeling studies yield conflicting results on whether southern Asia is a significant source of pollutants to the Arctic or not. Given the rapid industrialization of China, the increasing amounts of pollution being transported over long distances, and indications of increasing concentrations of absorbing aerosol in the Arctic more research is warranted to document the contribution of this source to Arctic Haze and to determine its climate impact on the Arctic. A warming climate has been forecast to result in large increases

in the areal extent of fires within Russian and Canadian Boreal forests (Stocks et al.1998). Hence, boreal forest fires are another source to be monitored to determine their impact on black carbon concentrations in atmospheric aerosol as well as black carbon that is deposited to snow and ice surfaces.

Other key atmospheric species have a distinct seasonality in the Arctic. There is evidence of the enrichment of halogens in Arctic air masses in late winter and spring. Since these compounds tend to peak later in the year, it is thought that they are produced photochemically. More research is required to partition their sources (e.g., anthropogenic, especially coal combustion vs. marine), to investigate their numerous and complex chemical pathways and, to assess their environmental impacts. Of special note is iodine, which shows a bimodal seasonal behavior, peaking in both spring and autumn (Sturges and Shaw, 1983).

The direct radiative effect of Arctic Haze has been estimated with 1-D radiative transfer models which find a warming in the atmosphere due to absorption of solar radiation and a concurrent cooling at the surface. These estimates are highly sensitive to the assumed properties of the aerosol in the haze. Despite the many research activities devoted to the characterization of Arctic Haze since the 1970s, measurements of Arctic aerosols are not extensive or well distributed in space or time which limits the accuracy of the estimates of both the direct and indirect radiative forcing. Treffeisen et al. (2004) have designed an approach based on cluster analysis for integrating aircraft, ground based, and long term data sets for use in 3-D climate models. The accurate evaluation of climate forcing by Arctic Haze requires such data sets coupled with 3-D climate models that consider both direct and indirect effects. In particular, three dimensional models are required to assess the complex feedbacks between aerosols, clouds, radiation, sea ice, and dynamic transport and to quantify climate forcing due to Arctic Haze (Girard et al., 2005).

Acknowledgements. This work was supported by the Atmospheric Constituents Program of the NOAA Office of Global Programs and the NOAA Arctic Research Office. We thank all members of the AMAP working group on Acidifying Pollutants, Arctic Haze, and Acidification in the Arctic for helpful discussions. This is PMEL contribution number 2945.

Albrecht, B.A., 1989. Aerosols, cloud microphysics, and fractional cloudiness, *Science*, 245, 1227-1230.

Barrie, L.A., 1996. Occurrence and trends of pollution in the Arctic troposphere. In: Wolff and Bales (eds.). Chemical exchange between the atmosphere and polar snow, pp. 93-130. Springer-Verslag, Heidelberg, NATO ASI Series 1: Global Environmental Change 43.

Barrie, L.A., R.M. Hoff, and S.M. Daggupaty, 1981. The influence of mid-latitudinal pollution sources on haze in the Canadian Arctic. *Atmos. Environ.* **15**, 1407-1419.

Blanchet J.-P. and R. List, 1987. Estimation of optical properties of Arctic haze using a numerical model, *Atmos.-Ocean*, **21**, 444 – 464.

Blanchet, J.-P. and E. Girard, 1995. Water-vapor temperature feedback in the formation of continental arctic air: implications for climate, *Sci. Tot. Environ.*, **160/161**, 793-802.

Bodhaine, B.A., 1989. Barrow surface aerosol: 1976 – 1986, *Atmos. Environ*., **23**, 2357 – 2369.

Bodhaine, B.A. and E.G. Dutton, 1993. A long-term decrease in Arctic haze at Barrow, Alaska, *Geophys. Res. Lett*., **20**(10), 947-950.

Borys, R.D., 1989. Studies of ice nucleation by arctic aerosol on AGASP-II, J. *Atmos. Chem.*, **9**, 169 – 185.

Bowling, S. A., and G. E. Shaw, 1992. The thermodynamics of pollution removal as an indicator of possible source areas for Arctic Haze, *Atmos. Env*., **26**, 2953-2961.

Brock, C.A., L.F. Radke, J.H. Lyons, and P.V. Hobbs, 1989. Arctic hazes in summer over Greenland and the North American Arctic, I, Incidence and origins, *J. Atmos. Chem*. **9**, 129 – 148.

Cess, C.R., 1983. Arctic aerosol: model estimates of the interactive influences upon the surface-troposphere radiation budget, *Atmos. Environ*., **17**, 2555-2564.

Clarke, A.D., 1989. In-stiu measurements of the aerosol size distributions, physicochemistry, and light absorption properties of Arctic haze, *J. Atmos. Chem*., **9**, 255-267.

Clarke, A.D. and K.J. Noone, 1985. Soot in the Arctic snowpack: A cause for perturbation in radiative transfer, *Atmos. Environ*., **19**, 2045-1053.

Coakley, J. A., Jr., and P. Chylek, 1975. The two-stream approximation in radiative transfer: including the angle of the incident radiation, *J. Atmos. Sci*., **32**, p. 409-418.

Curry, J.A., 1995. Interactions among aerosols, clouds, and climate of the Arctic Ocean, *Sci. Tot. Environ*., **160/161**, 777-791.

Curry, J.A. and G.F. Herman, 1985. Infrared radiative properties of Arctic stratus clouds, *J. Clim. Appl. Met*., **24**, 525-538.

Delene, D.J., and Ogren, J.A., 2002. Variability of aerosol optical properties at four North American surface monitoring sites, *J. Atmos. Sci*., **59**, 1135-1150.

Dibb, J.E., R.W. Talbot, S.I. Whitlow, M.C. Shipham, J. Winterle, J. McConnell, and R. Bales, 1996. Biomass burning signatures in the atmosphere and snow at Summit, Greenland: An event on 5 August 1994, *Atmos. Environ*., **30**, 553-561.

Douglas, T.A. and M. Sturm, 2004. Arctic haze, mercury, and the chemical composition of snow across northwestern Alaska, *Atmos. Environ*., **38**, 805-820.

Dutton, E.G., J.J. DeLuisi, and B.A. Bodhaine, 1984. Features of aerosol optical depth observed at Barrow, March 10-20, 1983, *Geophys. Res. Lett*., **11**, 385-388.

Eckhardt et al., 2003. The north Atlantic Oscillation controls air pollution transport to the Arctic, *Atmos. Chem. Phys*., **3**, 1769 – 1778.

Emery, C.A., R. Haberle, and T.P. Ackermann, 1992. A one-dimensional modeling study of carbonaceous haze effects on the springtime Arctic environment, *J. Geophys. Res*., **97**, 20599-20613.

Ferek, R.J., P.V. Hobbs, L.F. Radke, J.A. Herring, W.T. Sturges, and G.F. Cota, 1995. Dimethyl sulfide in the arctic atmosphere, *J. Geophys. Res*., **100**, 26093-26104.

Foster, J.S., J.W. Winchester, and E.G. Dutton, 1992. IEEE Trans. Geosci. Remote Sens., 30, 793-798.

Fromm, M., R. Bevilacqua, R. Servrancks, J. Rosen, J.P. Thayer, J. Herman, and D. Larko, 2005. Pyro-cumulonimbus injection of smoke to the stratosphere: Observations and impact of a super blowup in northwestern Canada on 3-4 August 1998, *J. Geophys. Res*., **110**, D08205, doi:10.1029/2004/JD005350.

Garrett, T.J., L.F. Radke, and P.V. Hobbs, 2002. Aerosol effects on the cloud emissivity and surface longwave heating in the Arctic, *J. Atmos. Sci*., **59**, 769-778.

Garrett, T.J., C. Zhao, X. Dong, G.G. Mace, and P.V. Hobbs, 2004. Effects of varying aerosol regimes on low-level Arctic stratus, *Geophys. Res. Lett.*, **31**, doi:10.1029/2004GL019928.

Gilbert, R.O., 1987. Statistical methods for environmental pollution monitoring. Van Nostrand Reinhold , New York.

Girard, E., J.-P. Blanchet, and Y. Dubois, 2005. Effects of arctic sulphuric acid aerosols on wintertime low-level atmospheric ice crystals, humidity and temperature at Alert, Nunavut, *Atm. Res.*, **73**, 131-148.

Greenaway, K.R., 1950. Experiences with Arctic flying weather, Royal Meteorological Society Canadian Branch (Nov. 30, 1950), Toronto, Ontario.

Hansen, A.D.A. and H Rosen, 1984. Vertical distribution of particulate carbon, sulphur and bromine in the Arctic haze and comparison with ground-level measurements at Barrow, Alaska. *Geophys. Res. Lett*. **11,** 381 – 384.

Hansen, J. and L. Nazarenko, 2004. Soot climate forcing via snow and ice albedos, *Proc. Natl. Acad. Sci.*, **101**(2), 423-428.

Heidam, N.Z., J. Christensen, P. Wahlin, and H. Skov, 2004. Arctic atmospheric contaminants in NE Greenland: levels, variations, origins, transport, transformations, and trends 1990 – 2001. *Sci. Tot. Environ.*, **331**(1-3), 5-28.

Heintzenberg, J., 1980. Particle size distribution and optical properties of Arctic haze. *Tellus*, **32B**, 251 – 260.

Heintzenberg, J. and S. Larssen, 1983. SO_2 and SO_4 in the Arctic. Interpretation of observations at three Norwegian Arctic-Subarctic stations, *Tellus*, **35B**, 255 – 265.

Heintzenberg, J. et al., 2003. Arctic Haze over Central Europe, *Tellus*, **55B**, 796-807.

Herber, A. et al., 2002. Continuous day and night aerosol optical depth observations in the Arctic between 1991 and 1999, *J. Geophys. Res.*, **107**(D10), 10.1029/2001JD000536.

Hillamo, R.E., V.-M. Kerminen, W. Maenhaut, J.-L. Jaffrezo, S. Balachandran and C.I. Davidson, 1993. Size distributions of atmospheric trace elements at Dye 3, Greenland – 1. Distribution characteristics and dry deposition velocities. *Atmos. Environ*. **27A**(17-18): 2787-2803.

Hobbs, P.V. and A.L. Rangno, 1998. Microstructures of low and middle-level clouds over the Beaufort Sea, *Q.J.R. Met. Soc*., **124**, 2035-2071.

Hoff, R.M., 1988. Vertical structure of Arctic haze observed by Lidar. *J. Appl. Met*. **27**,125 – 139.

Hoff, R.M., W.R. Leaitch, P. Fellin, and L.A. Barrie, 1983. Mass-size distributions of chemical constituents of the winter Arctic aerosol. *J. Geophys. Res*. **88**: 10947 – 10956.

Hopper, J.E., D.E.J. Worthy, L.A. Barrie, and N.B.A. Trivett, 1994. Atmospheric observations of aerosol black carbon, carbon dioxide and methane in the High Arctic. *Atmos. Environ*. **28**: 3047 – 3054.

Hurrell, J.W. and H. Van Loon, 1997. Decadal variations in climate associated with the North Atlantic Oscillation, *Clim. Change* **36**: 301 – 326.

Iversen, T. and E. Joranger, 1985. Arctic air pollution and large scale atmospheric flows, *Atmos. Environ*., **19**, 2099 – 2108.

Jaffe, D., T. Iversen, and G. Shaw, 1995. Comment on "A long term decrease in arctic haze at Barrow, Alaska" by B.A. Bodhaine and E.G. Dutton, *Geophys. Res. Lett.*, **22**(6), 739-740.

Kahl, J.D. and A.D.A. Hansen, 1989. Determination of regional sources of aerosol black carbon in the Arctic. *Geophys. Res. Lett*. **16**(4): 327 – 330.

Kahl, J.D. 1990. Characteristics of the low-level temperature inversion along the Alaskan Arctic coast, *Int. J. Climatol*. **10**, 537 – 548.

Kawamura, K., H. Kasukabe, and L.A. Barrie, 1996. Source and reaction pathways of dicarboxylic acids, ketoacids, and dicarbonyls in Arctic aerosols: One year of observations. *Atmos. Environ*. **30**, 1709 – 1722.

Klonecki, A., P. Hess, L. Emmons, L. Smith, J. Orlando, and D. Blake, 2003. Seasonal changes in the transport of pollutants into the Arctic troposphere- model study. *J. Geophys. Res*., **108**, 8367. doi:10.1029/2002JD002199.

Koch, D. and J. Hansen, 2004. Distant origins of Arctic black carbon: A Goddard Institute for Space Studies ModelE experiment, *J. Geophys. Res.,* **100**, D04204, doi:10.1029/2004JD005296.

Leaitch, W.R., R.M. Hoff, S. Melnichuk and A. Hogan, 1984. Some physical and chemical properties of the Arctic winter aerosol in northeastern Canada. *J. Clim. Appl. Met.* **23**:916 – 928.

Leaitch, W.R., R.M. Hoff, and J.L. MacPherson, 1989. Airborne and Lidar measurements of aerosol and cloud particles in the troposphere over Alert Canada in April 1986. *J. Atmos. Chem*. **9**(1-3): 187 – 212.

Leighton, H., 1983. Influence of the Arctic haze on the solar radiation budget. *Atmos. Environ*., **17**, 2065-2068.

Li, S.M. and L.A. Barrie, 1993. Biogenic sulphur aerosols in the Arctic troposphere. 1. Contributions to sulphate. *J. Geophys. Res*. **98**D: 20613 – 20622.

Macdonald, R.W., T. Harner, and J. Fyfe, 2005. Recent climate change in the Arctic and its impact on contaminant pathways and interpretation of temporal trend data, *Sci. Tot. Environ.* **342**: 5-86.

MacCraken, M.C., R.D. Cess, and G. L. Potter, 1986. Climatic effects of anthropogenic Arctic aerosols: An illustration of climatic feedback mechanisms with one-and two-dimensional climate models, *J. Geophys. Res*., **91**, 14445-14450.

Masclet, P., V. Hoyau, J.L. Jaffrezo, and H. Cachier, 2000. Polycyclic aromatic hydrocarbon deposition on the ice sheet of Greenland. Part 1: Superficial snow, *Atmos. Environ*., **34**, 3195 – 3207.

Meijer, S.N., W.A. Ockenden, A. Sweetman, K. Breivik, J.O. Grimalt, and K.C. Jones, 2003. Global distribution and budget of PCBs and HCB in background surface

soils: Implications for sources and environmental processes, *Environ. Sci. Technol*., **37**, 667 – 672.

Mendonca, B.G., J.J. DeLuisi, and J.A. Schroeder, 1981. Arctic Haze and perturbation in the solar radiation fluxes at Barrow, Alaska, Proceedings from the 4th Conference on Atmospheric Radiation. Atm. Met. Sco., Toronto, Ontario, Canada, pp. 95-96.

Mitchell, M., 1956. Visual range in the polar regions with particular reference to the Alaskan Arctic. *J. Atmos. Terrestrial Phys*., Special Suppl.: 195-211.

Noone, K.J. and A.D. Clarke, 1988. Soot scavenging measurements in Arctic snowfall. *Atmos. Environ*. **22**(12): 2773 – 2779.

Ottar, B., Y. Gotaas, O. Hov, T. Iversen, E. Joranger, M. Oehme, J. Pacyna, A. Semb, W. Thomas, and V. Vitolas, 1986. Air pollutants in the Arctic. Final report of a research programme conducted on the behalf of British Petroleum, Ltd. The Norwegian Institute of Air Research, Kjeller, Norway, NILU OR 30/86., 80p.

Pacyna, J.M., V. Vitolis and J.E. Hanssen, 1984. Size differentiated composition of the Arctic aerosol at Ny Alesund Zeppelin. *Atmos. Environ*. **18**: 2447 – 2459.

Pacyna, J.M. and B. Ottar, 1988. Vertical distribution of aerosols in the Norwegian Arctic. *Atmos. Environ*. **22**(10): 2213-2223.

Penkett, S.A., N.J. Blake, P. Lightman, A.R.W. Marsh, P. Anwyl, , and G. Butcher, 1993. The seasonal variation of nonmethane hydrocarbons in the free troposphere over the North Atlantic Ocean: Possible evidence for extensive reaction of hydrocarbons with the nitrate radical, *J. Geophys. Res.*, **98**, 2865-2885.

Polissar, A.V., Hopke, P.K., Paatero, P., Malm, W.C., Sisler, J.F., 1998. Atmospheric aerosol over Alaska 2. Elemental composition and sources, *J. Geophys. Res*., **103**, 19045-19057.

Polissar, A.V., Hopke, P.K., Harris, J.M., 2001. Source regions for atmospheric aerosol measured at Barrow, Alaska, *Environ. Sci. Tech.*, **35**, 4214-4226.

Porch, W.M. and M.C. MacCracken, 1982. Parametric study of the effects of Arctic soot on the solar radiation, *Atmos. Environ*., **16,** 1365-1371.

Pueschel, R.F. and S.A. Kinne, 1995. Physical and radiative properties of Arctic atmospheric aerosols, *Sci. Tot. Environ.*, **161**, 811-824.

Quinn, P.K., T.S. Bates, T.L. Miller, D.J. Coffman, J.E. Johnson, J. M. Harris, J.A. Ogren, G. Forbes, T.L. Anderson, D.S. Covert, and M.J. Rood, 2000. Surface Submicron Aerosol Chemical Composition: What Fraction is Not Sulfate? *J. Geophys. Res.*, **105**, 6785 – 6806.

Quinn, P.K., T.L. Miller, T.S. Bates, J.A. Ogren, E. Andrews, and G.E. Shaw, 2002. A three-year record of simultaneously measured aerosol chemical and optical properties at Barrow, Alaska, *J. Geophys. Res*., **107**(D11), 10.1029/2001JD001248.

Radke, F.S., J.H. Lyons, D.A. Hegg, P.V. Hobbs, and I.H. Bailey, 1984. Airborne observations of arctic aerosols, I, Characteristics of arctic haze. *Geophys. Res. Lett*. **11**, 393-396.

Rahn, K.A., 1989. Proceedings of the International Symposium on Arctic Air Chemistry, *Atmos. Environ*., **23**(11): 2345 – 2347.

Rahn, K.A., R. Borys, and G.E. Shaw, 1977. The Asian source of Arctic haze bands, *Nature,* **268**, 713-715.

Rahn, K.A. and R.J. MacCaffrey, 1979. Long range transport of pollution aerosol to the Arctic. A problem without borders. Proc. WMO Symp. On the long range transport of pollutants and its relations to general circulation including stratospheric/tropospheric exchange processes, pp. 25 – 25, Sofia, 1-5 Oct 1980. WMO No. 538.

Rahn, K. A., R. D. Borys and G. E. Shaw, 1981. Asian desert dust over Alaska: Anatomy of an Arctic Haze Episode, Desert Dust. In: Origin, Characteristic and Effect on Man, Pewe, T. (ed. 37-70, Special paper No. 186, The Geol. Soc. Am.,Boulder, CO.

Ricard, V., J.-L. Jaffrezo, V.-M. Kerminen, R.E. Hillamo, M. Sillanpaa, S. Ruellan, C. Liousse, and H. Cachier, 2002. Two years of continuous aerosol measurements in northern Finland. *J. Geophys. Res*. **107**(D11), 10.1029/2001JD000952.

Ritter, C., J. Notholt, J. Fischer, and C. Rathke, 2005. Direct thermal radiative forcing of tropospheric aerosol in the Arctic measured by ground based infrared spectrometry, *Geophys. Res. Lett*., **32**, L23816, doi:10.1029/2005GL024331.

Salmi, T., Maatta, A., Anttila, P., Ruoho-Airola, T., and Amnell, T., 2002. Detecting trends of annual values of atmospheric pollutants by the Mann-Kendall test and Sen's slope estimates – the Excel template application MAKESENS, Publications on Air Quality, no. 31, FMI-AQ-31, FMI, Helsinki, Finland.

Scheuer, E., R.W. Talbot, J.E. Dibb, G.K. Seid, L. DeBell, and B. Lefer, 2003. Seasonal distributions of fine aerosol sulfate in the North American Arctic basin during TOPSE. *J. Geophys. Res*., **108**(D4), 8370, doi:10.1029/2001JD001364.

Sen P.K., 1968. Estimates of the regression coefficient based on Kendall's tau. J. of the American Statistical Association, 63, 1379-1389.

Sharma, S., D. Lavoue, H. Cachier, L.A. Barrie, S.L. Gong, 2004. Long-term trends of the black carbon concentrations in the Canadian Arctic, *J. Geophys. Res*., **109**, doi:10.1029/2003JD004331.

Sharma, S., E. Andrews, L.A. Barrie, J.A. Ogren, D. Lavoue, 2006. Variations and sources of the equivalent black carbon in the High Arctic Revealed by Long Term Observations at Alert and Barrow : 1989 – 2003, *J. Geophys. Res., in press.*

Shaw, G. E., 1975. The vertical distribution of atmospheric aerosols at Barrow, Alaska, *Tellus*, **27**, 39-50.

Shaw, G.E., 1981. Eddy diffusion transport of Arctic pollution from the mid-latitudes: a preliminary model, *Atmos. Environ.*, **15**, 1483 – 1490.

Shaw, G. E., 1983. Evidence for a central Eurasian source area of Arctic Haze in Alaska, *Nature*, **299**, 815-818.

Shaw, G.E., 1984. Microparticle size spectrum of Arctic haze. *Geophys. Res. Lett.* **11**: 409 – 412.

Shaw, G. E., 1987. Aerosols as climate regulators: A climate biosphere linkage? *Atmos. Env*., **21**, 985-1086.

Shaw, The Arctic Haze phenomenon, 1995. *Bull. Am. Met. Soc*., **76**, 2403-2413.

Shaw, G.E. and G. Wendler, 1972. Atmospheric turbidity measurements at McCall Glacier in northeast Alaska, Conference Proc. On Atmospheric Radiation, pp. 181 – 187, Fort Collins, Colorado. Am. Met. Soc., Boston.

Shaw, G.E. and K. Stamnes, 1980. Arctic haze: perturbation of the Polar radiation budget, *Am. N.Y. Acad. Sci*, **338**, 533 – 539.

Shaw, G.E., K. Stamnes, and Y.X. Hu, 1993. Arctic haze: Perturbation to the radiation field, Meteorol. *Atmos. Phys*., **51**, 227-235.

Shaw, G. E., 1981. Aerosol chemical components in Alaska air masses 1. Aged Pollution and II Sea Salt and Marine Product, *J. Geophy. Res*., **96**, 22,357-22,372.

Sirois, A. and L.A. Barrie, 1999. Arctic lower tropospheric aerosol trends and composition at Alert, Canada: 1980 – 1995, *J. Geophys. Res*., **104**, 11599 – 11618.

Stocks, B.J. et al., 1998. Climate change and forest fire potential in Russian and Canadian boreal forests, *Clim. Change*, **38**, 1 – 13.

Stohl, A., 2006. Characteristics of atmospheric transport into the Arctic troposphere, *J. Geophysical Res*., **111**, D11306, doi:10.1029/2005JD006888.

Stone, R.S., 2002a, Earlier spring snowmelt in northern Alaska as an indicator of climate change, *J. Geophys. Res*., **107**, d104089, 10.1029/2000JD000286.

Stone, R.S., 2002b. Monitoring aerosol optical depth at Barrow, Alaska and South Pole; Historical overview, recent results, and future goals, Proceedings of the 9th Workshop Italian Research on Antarctic Atmosphere, Rome, Italy, 22 – 24, October, 2001, edited by M. Colacino, pp. 123 – 144, Ital. Phys. Soc., Bologna, Italy.

Sturges, W.T. and L.A. Barrie, 1988. Chlorine, bromine, and iodine in Arctic aerosols, *Atmos. Environ*., **22**, 1179 – 1194.

Sturges, W. T. and G. E. Shaw, 1983. Halogens in aerosols in central Alaska, *Atmos. Environ*., **27,** 2969-2977.

Treffeisen, R. et al., 2004. Interpretation of Arctic aerosol properties using cluster analysis applied to observations in the Svalbard area, *Tellus*, **56B**, 457-476.

Trivett, N.B.A., L.A. Barrie, J.P. Blanchet, R.M. Bottenheim, R.M. Hoff and R.E. Mickle, 1989. An experimental investigation of Arctic haze at Alert, N.W.T., March 1985. *Atmos. Ocean*. **26**: 341 – 376.

Twomey, S., 1977. The influence of pollution on the shortwave albedo of clouds, *J. Atmos. Sci.,* **34**, 1149-1152.

Twomey, S., 1991. Aerosols, clouds and radiation, *Atmos. Environ*., **25A**, 2435.

Valero, F. P. J., and T. P. Ackerman, 1986. Arctic haze and radiation balance, in Arctic Air Pollution, B. Stonehouse, Ed., Cambridge Press, 121-133.

Valero, F.P.J., T.P. Ackerman, and W.J.R. Gore, 1989. The effects of the arctic haze as determined from airborne radiometric measurements during AGASP II, J. *Atmos. Chem.*, **9**, 225-244.

Vestreng, V. 2003. Review and revision of emission data reported to CLRTAP. EMEP/MSC-W Note1. Norwegian Meteorological Institute.

Waggoner, A.P. and R.E. Weiss, 1980. Comparison of the fine particle mass concentration and light scattering extinction in ambient aerosol. *Atmos. Environ*. **14**: 623 – 626.

Wania, F., 2003. Assessing the potential of persistent organic chemicals for long-range transport and accumulation in polar regions, *Environ. Sci. Technol*., **37**, 1344 – 1351.

Warren, S.G. and W.J. Wiscombe, 1980. A model for the spectral albedo of snow. II. Snow containing atmospheric aerosols, *Aer. Sci. Tech*. **4**, 31-43.

Wiscombe, W. J., and G. W. Grams, 1976. The backscattered fraction in two-stream approximations, *J. Atmos Sci*., **33**, 2440-2451.

Zhang, T., K. Stamnes, and S.A. Bowling, 1996. Impact of clouds on surface radiative fluxes and snowmelt in the Arctic and subarctic, *J. Clim*. **9**, 2110-2123.

Table 1. Change in monthly average sulfate concentrations for March and April. Significance of the trend, Sen's slope estimate, and percent change per period are listed.

Station	Species	Period	α[a]	Slope[b]	Change per period %
Alert	nss $SO_4^=$	Mar, 1981 - 2002	0.01	-0.066	- 66
		Apr, 1981 – 2003	0.001	-0.079	- 71
		Mar, 1990 - 2002	0.001	-0.088	-59
		Apr, 1990 – 2003	0.01	-0.086	- 63
Nord	$SO_4^=$	Mar, 1990 - 2002			
		Apr, 1990 - 2002			
Zeppelin	$SO_4^=$	Mar, 1990 - 2003	0.1	-0.094	- 33
		Apr, 1990 - 2003	0.1	-0.079	- 27
Barrow	nss $SO_4^=$	Mar, 1998 - 2004			
		Apr, 1998 - 2004			
Karasjok	$SO_4^=$	Mar, 1978 - 2003	0.001	-0.044	- 80
		Apr, 1978 – 2003	0.001	-0.021	- 59
		Mar, 1990 - 2003	0.1	-0.017	- 40
		Apr, 1990 – 2003	0.01	-0.025	- 48
Svanvik	$SO_4^=$	Mar, 1993 - 2000			
		Apr, 1993 - 2000			
Janiskoski	$SO_4^=$	Mar, 1991 - 2002			
		Apr, 1991 - 2002			
Oulanka	$SO_4^=$	Mar, 1990 - 2002	0.1	-0.034	- 45
		Apr, 1990 - 2002	0.01	-0.043	- 56

[a]Significance level, α, of the Mann-Kendall test. A significance level of 0.001 indicates a 0.1% probability of no trend. No value indicates a significance level > 0.1.

[b]Sen's nonparametric method was used to estimate the slope of the existing trend as change per year ($\mu g\ S\ m^{-3}\ yr^{-1}$).

Table 2. Change in monthly average nitrate concentrations for March and April. Significance of the trend, Sen's slope estimate, and percent change per period are listed.

Station	Species	Period	α[a]	Slope[b]	Change per period %
Alert	NO_3^-	Mar, 1981 - 2003			
		Apr, 1981 – 2003	0.1	0.0006	67
		Mar, 1990 - 2003	0.05	0.0008	50
		Apr, 1990 – 2003			
Barrow	NO_3^-	Mar, 1998 - 2004			
		Apr, 1998 - 2004			

[a]Significance level, α, of the Mann-Kendall test. A significance level of 0.001 indicates a 0.1% probability of no trend. No value indicates a significance level > 0.1.

[b]Sen's nonparametric method was used to estimate the slope of the existing trend as change per year (μg N m^{-3} yr^{-1}).

Table 3. Change in monthly average light scattering and absorption at Barrow and black carbon (BC) at Alert for March and April. Significance of the trend, Sen's slope estimate, and percent change per period are listed.

Station	Species	Period	α[a]	Slope[b]	Change per period %
Barrow	σ_{sp}[c]	Mar, 1977 – 2006	0.01		
		Apr, 1977 – 2006			
		Mar, 1982 - 1996	0.01	-5.7 E-07	- 42
		Apr, 1982 - 1996	0.01	-6.6 E-7	- 56
		Mar, 1997 – 2006	0.05	7.8 E-07	46
		Apr, 1997 – 2006			
Barrow	σ_{ap}[c]	Mar, 1988 – 2006	0.1	-3.9 E-08	-61
		Apr, 1988 – 2006			
		Mar, 1988 – 1996			
		Apr, 1988 – 1996			
		Mar, 1997 – 2006			
		Apr, 1997 - 2006			
Alert	BC	Mar, 1990 - 2001	0.001	-17	- 88
		Apr, 1990 - 2001	0.05	-8.3	-63
		Mar, 1997 - 2001	0.1	-3.9	-20
		Apr, 1997 - 2001			

[a]Significance level, α, of the Mann-Kendall test. A significance level of 0.001 indicates a 0.1% probability of no trend. No value indicates a significance level > 0.1.

[b]Sen's nonparametric method was used to estimate the slope of the existing trend as change per year (Mm^{-1} yr^{-1} for scattering and absorption, ng m^{-3} yr^{-1} for black carbon).

[c]Sub-10 micrometer aerosol.

Table 4. Calculated Radiative Forcing of Arctic Haze at the Top of the Atmosphere and at the Surface in W m^{-2}.

A[a]	t[b]	ω[c]	β[d]	μ[e]	H[f]	å[g]	ΔF TOA[h]	ΔF Surface[i]
0.92	0.12	0.94	0.26	0.46	1	1.5	2.5	-0.93

[a]Surface albedo based on measurements over a snow-covered surface in April. The measured range of A was 0.85 to 0.95 for wavelengths between 400 and 650 nm.
[b]Aerosol optical depth at 500 nm based on a weighted mean from several measurement sources (Valero and Ackerman, 1983; Stone, 2002b). A power law form for the wavelength dependence of τ was assumed. An Ångström exponent of 1.5 was used in all calculations representing submicrometer particles based on measurements at Barrow (Delene and Ogren, 2002).
[c]Single scattering albedo at 550 nm based on measurements at Barrow reported by Delene and Ogren (2002). No wavelength dependence incorporated into the calculations because of uncertainties in the wavelength variation, size, and composition of the aerosol.
[d]Fraction of scattered radiation that is scattered into the upward hemisphere. Based on nephelometer measurements of the hemispheric backscattered fraction, b, and the use of the Henyey-Greenstein phase function to calculate β from b (Wiscombe and Grams, 1976 ; Sheridan and Ogren, 1999). A b of 0.105 was used based on measurements at Barrow (Delene and Ogren, 2002).
[e]Cosine of the noon solar zenith angle for April 15 at the latitude of Barrow.
[f]Vertical thickness of the haze layer in km.
[g]Ångström exponent or power law coefficient of aerosol optical depth.
[h]Radiative forcing at the top of atmosphere in W m^{-2}
[i]Radiative forcing at the surface in W m^{-2}.

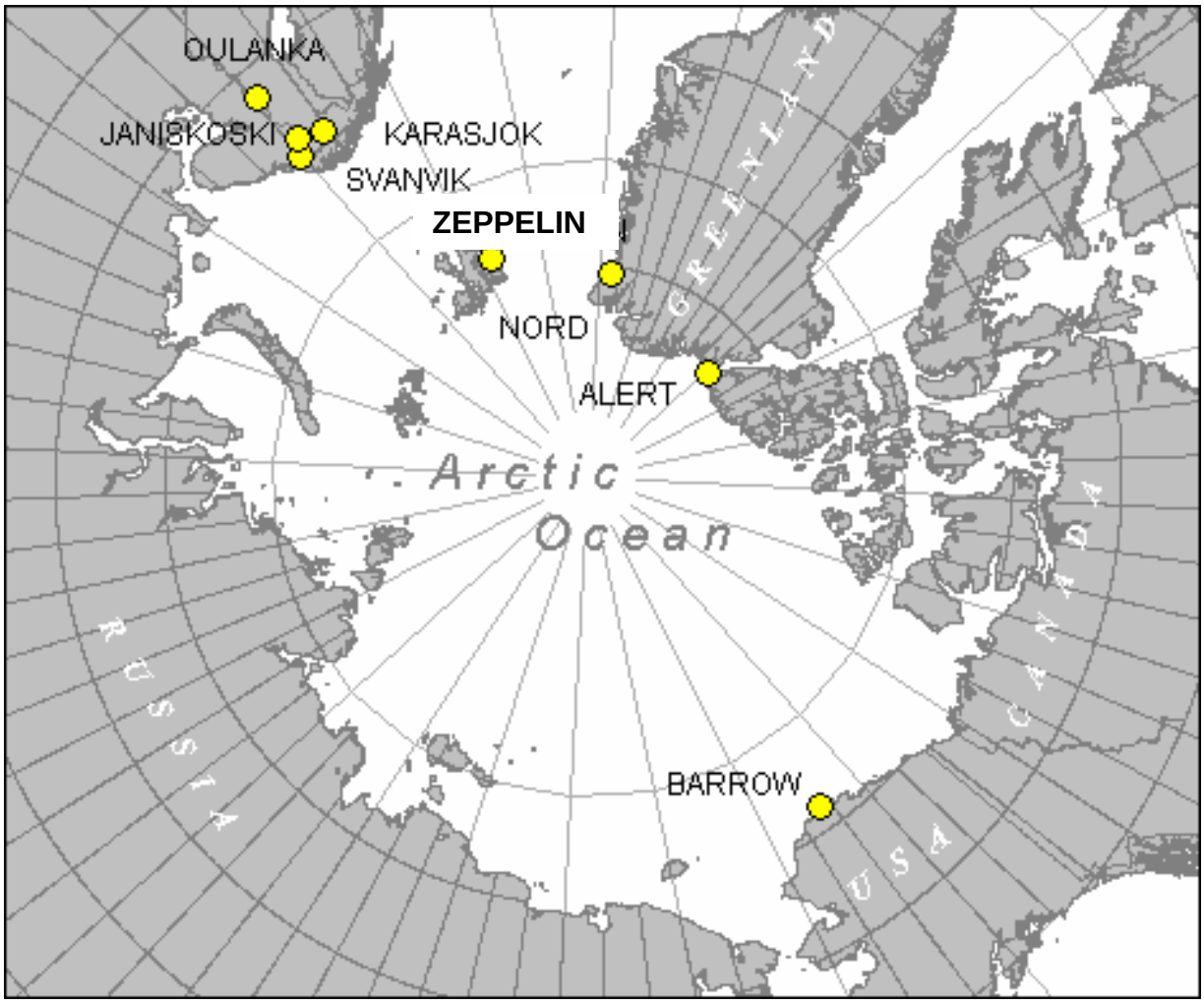

Figure 1. Arctic sampling station locations.

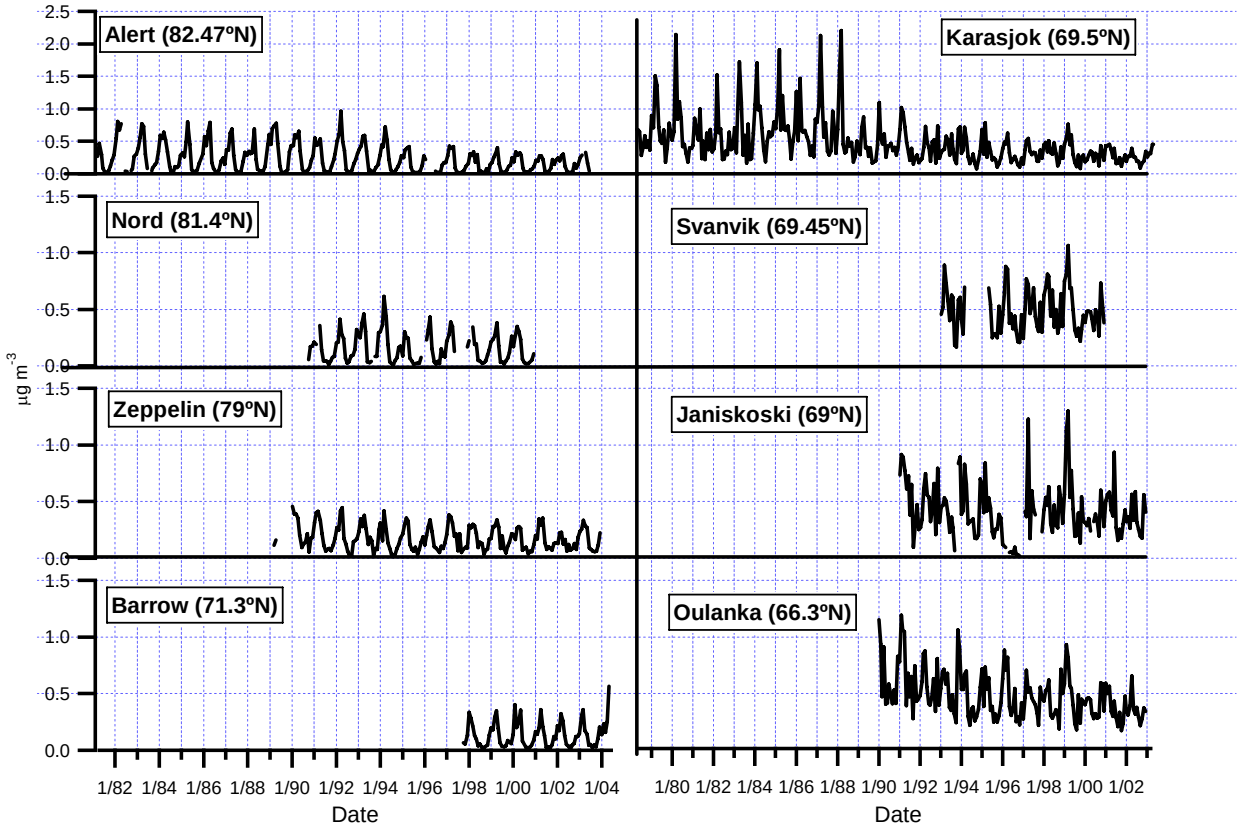

Figure 2. Time series of monthly averaged particulate sulfate concentrations in µg S m^{-3} for eight Arctic monitoring sites. Data made available for Alert by the Canadian National Atmospheric Chemistry (NAtChem) Database and Analysis System, for Barrow by NOAA PMEL (http://saga.pmel.noaa.gov/data/), and for the other stations by EMEP (http://www.emep.int/).

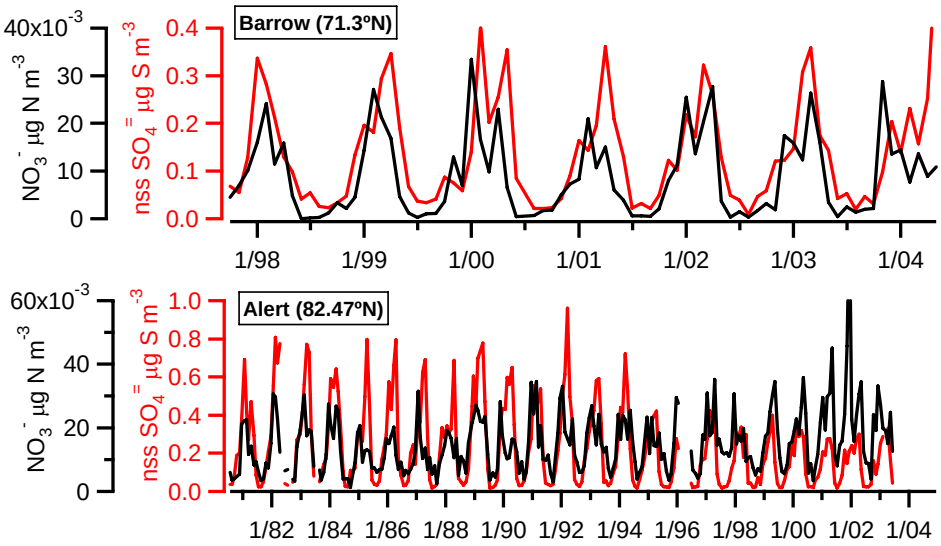

Figure 3. Time series of monthly averaged particulate sulfate and nitrate concentrations in µg S m^{-3} and µg N m^{-3}, respectively, for a) Barrow, Alaska and b) Alert, Canada. Data made available for Alert by the Canadian National Atmospheric Chemistry (NAtChem) Database and Analysis System and for Barrow by NOAA PMEL (http://saga.pmel.noaa.gov/data/).

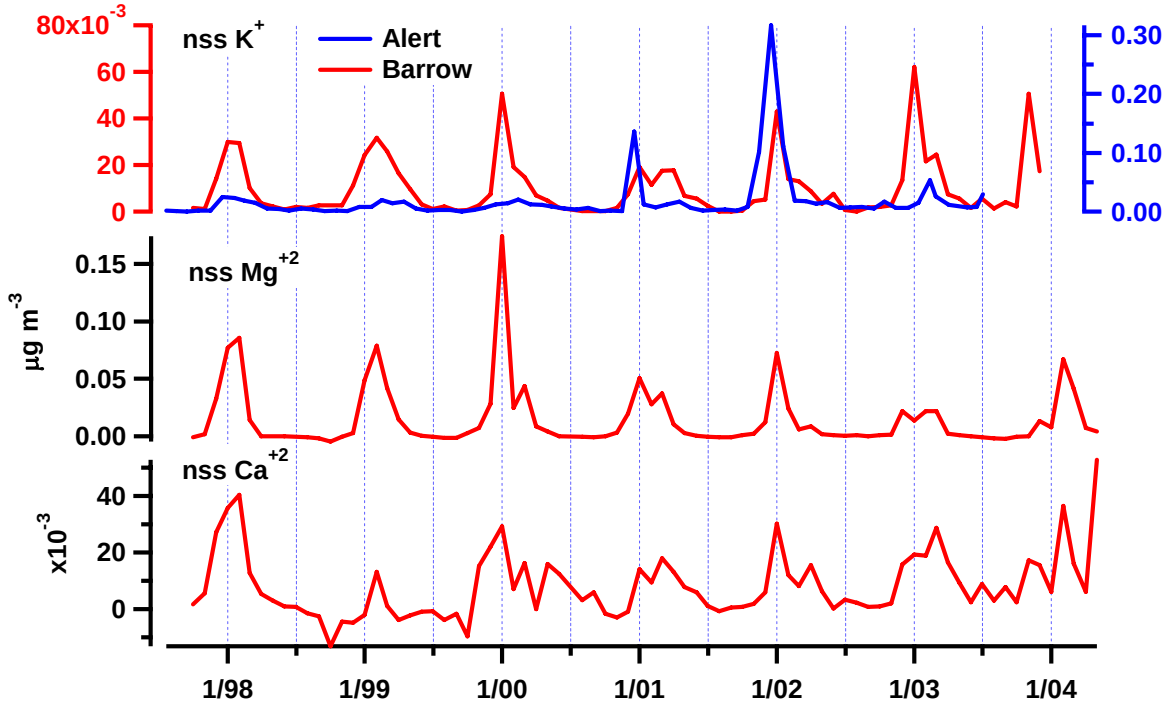

Figure 4. Time series of monthly averaged nss K^{+}, nss $Mg^{+2,}$ and nss Ca^{+2} in µg m^{-3} for Barrow, Alaska and Alert, Canada. Alert nss K^{+} are available from 1980 to 2003.Data made available for Alert by the Canadian National Atmospheric Chemistry (NAtChem) Database and Analysis System and for Barrow by NOAA PMEL (http://saga.pmel.noaa.gov/data/).

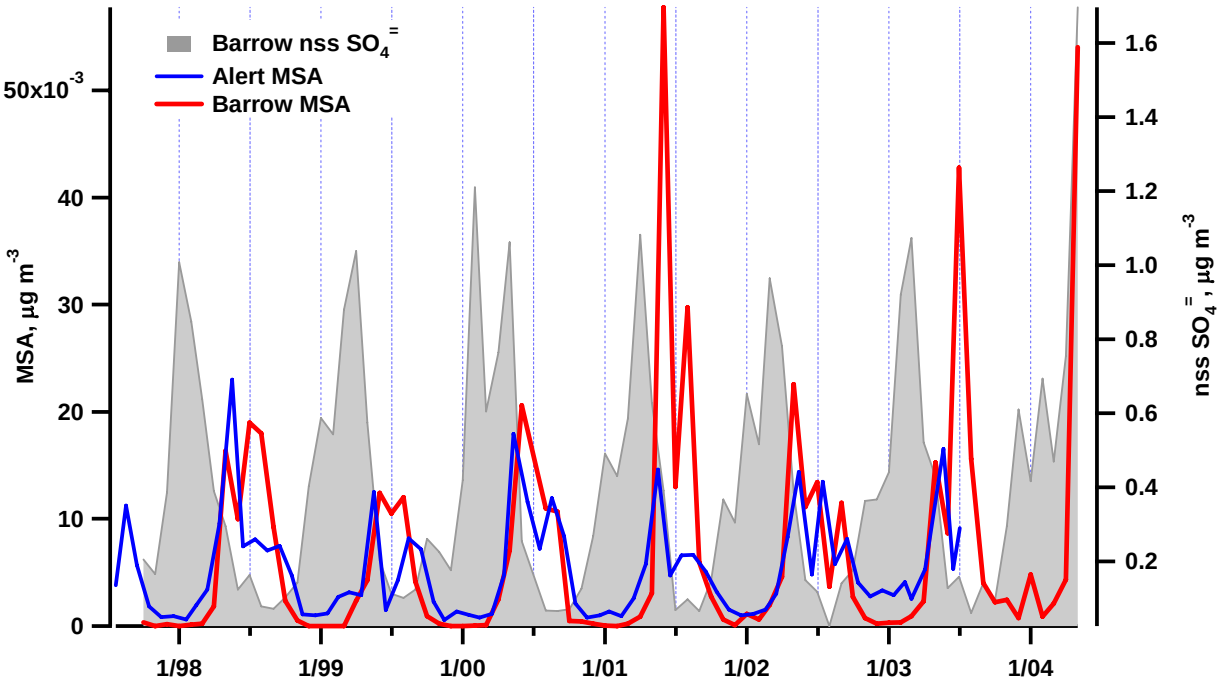

Figure 5. Time series of monthly averaged MSA in µg m^{-3} for Barrow, Alaska and Alert, Canada. Barrow nss $SO_4^=$ is shown for the seasonal contrast. Alert MSA data are available from 1980 to 2003. Data made available for Alert by the Canadian National Atmospheric Chemistry (NAtChem) Database and Analysis System and for Barrow by NOAA PMEL (http://saga.pmel.noaa.gov/data/).

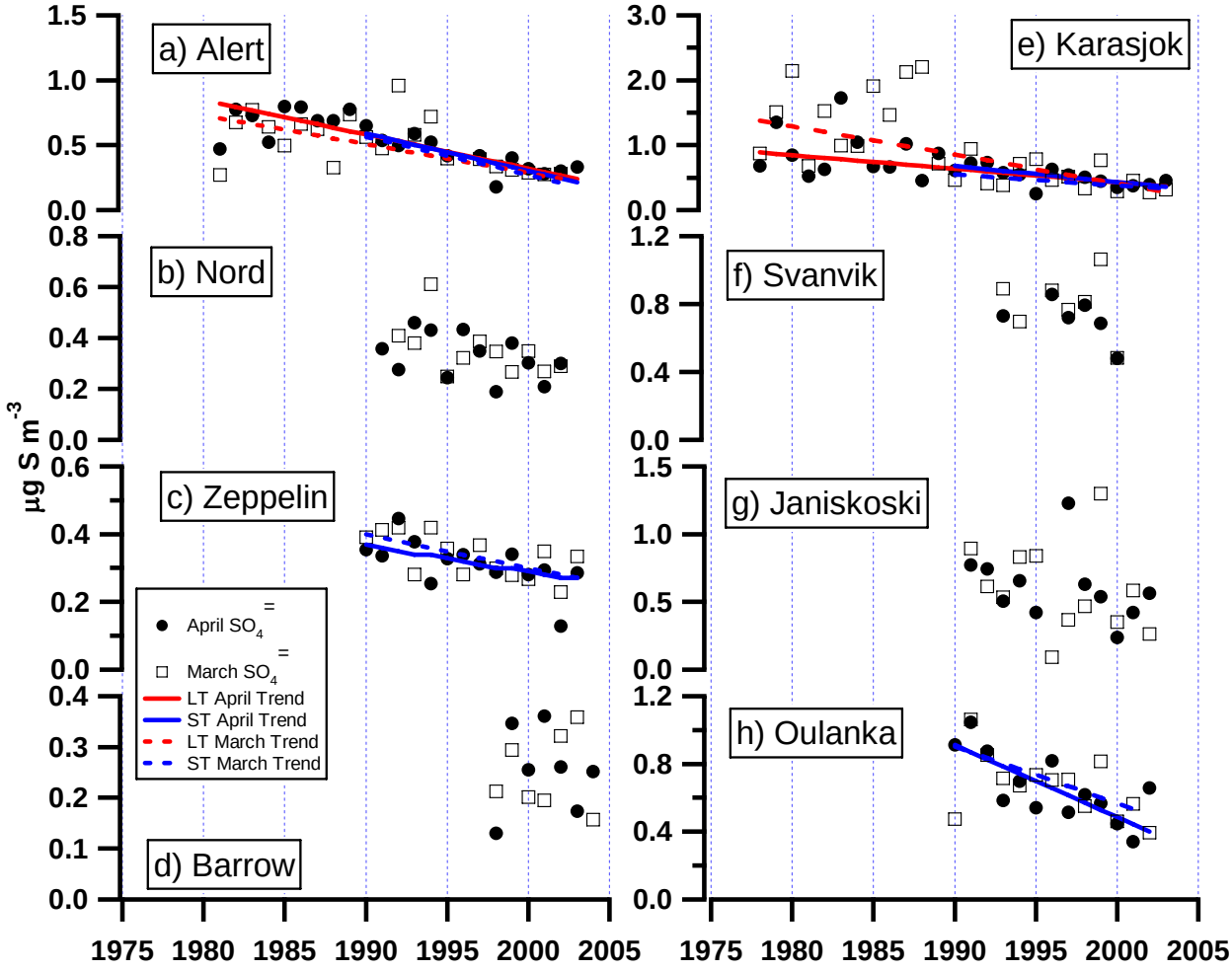

Figure 6. Monthly averaged concentrations in μg S m^{-3} of sulfate for March and April. Red lines indicate the Sen's slope estimate for the long term (LT) trend (approximately 1980 through the available data). Blues lines indicate the Sen's slope estimate for the short term (ST) trend (approximately 1990 through the available data). Trend lines are not shown if the significance for the trend according to the Mann-Kendall test is $\alpha > 0.1$. Data made available for Alert by the Canadian National Atmospheric Chemistry (NAtChem) Database and Analysis System, for Barrow by NOAA PMEL (http://saga.pmel.noaa.gov/data/), and for the other stations by EMEP (http://www.emep.int/).

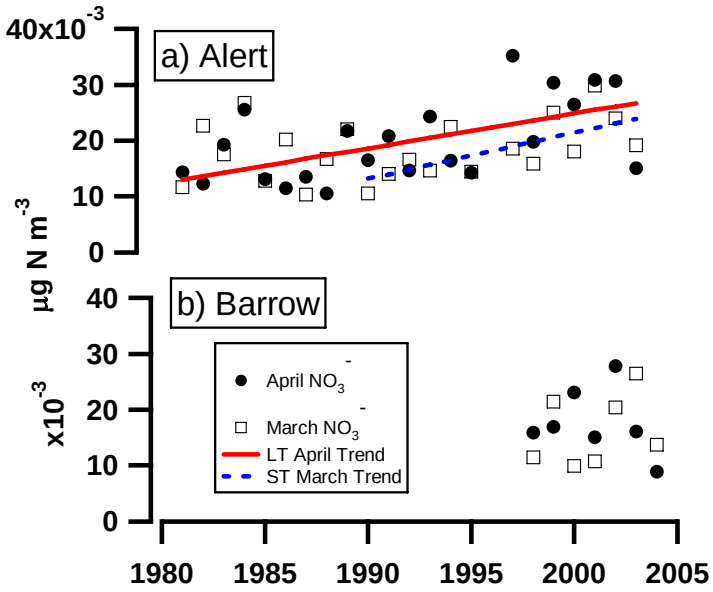

Figure 7. Monthly averaged concentrations in µg N m^{-3} of nitrate for March and April. Red lines indicate the Sen's slope estimate for the long term (LT) trend (approximately1980 through the available data). Blues lines indicate the Sen's slope estimate for the short term (ST) trend (approximately 1990 through the available data). Trend lines are not shown if the significance for the trend according to the Mann-Kendall test is $\alpha > 0.1$. Data made available for Alert by the Canadian National Atmospheric Chemistry (NAtChem) Database and Analysis System, for Barrow by NOAA PMEL (http://saga.pmel.noaa.gov/data/).

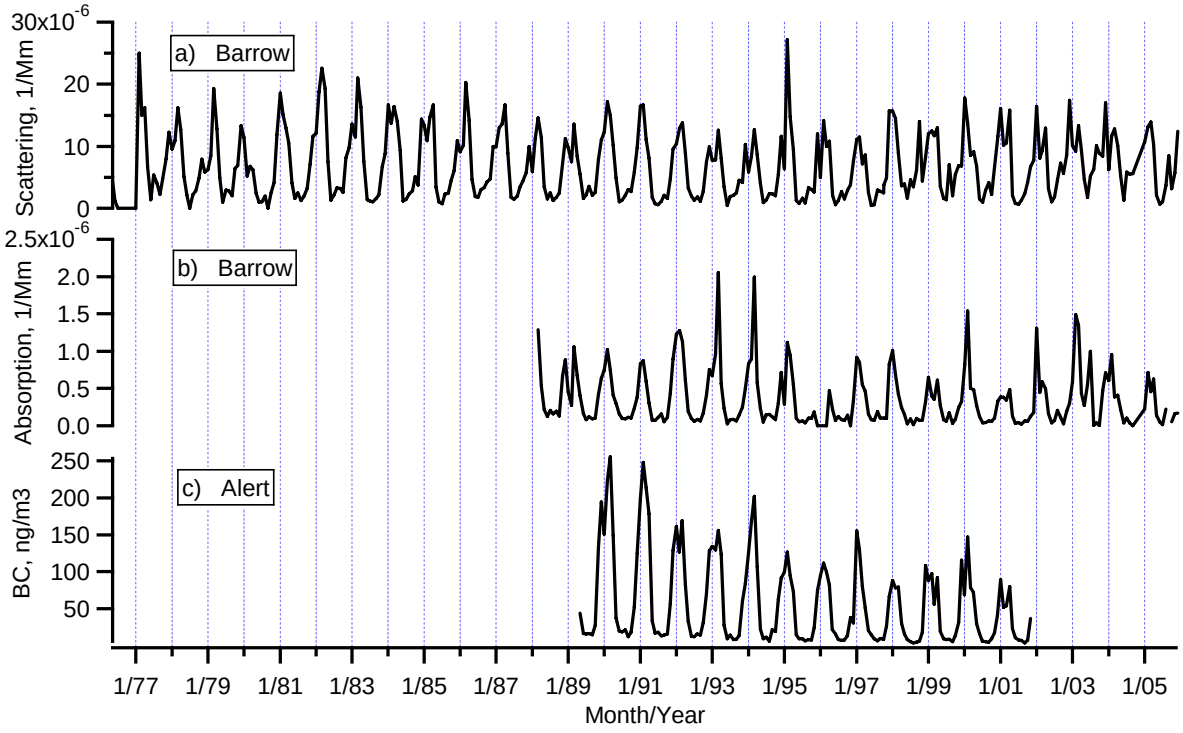

Figure 8. Monthly averaged a) light scattering and b) absorption at 550 nm by sub-10 micron aerosol at Barrow, Alaska (1/Mm) and c) black carbon mass concentration (ng/m3) at Alert, Canada. Data made available for Barrow by NOAA GMD and for Alert by the Canadian National Atmospheric Chemistry (NAtChem) Database and Analysis System.

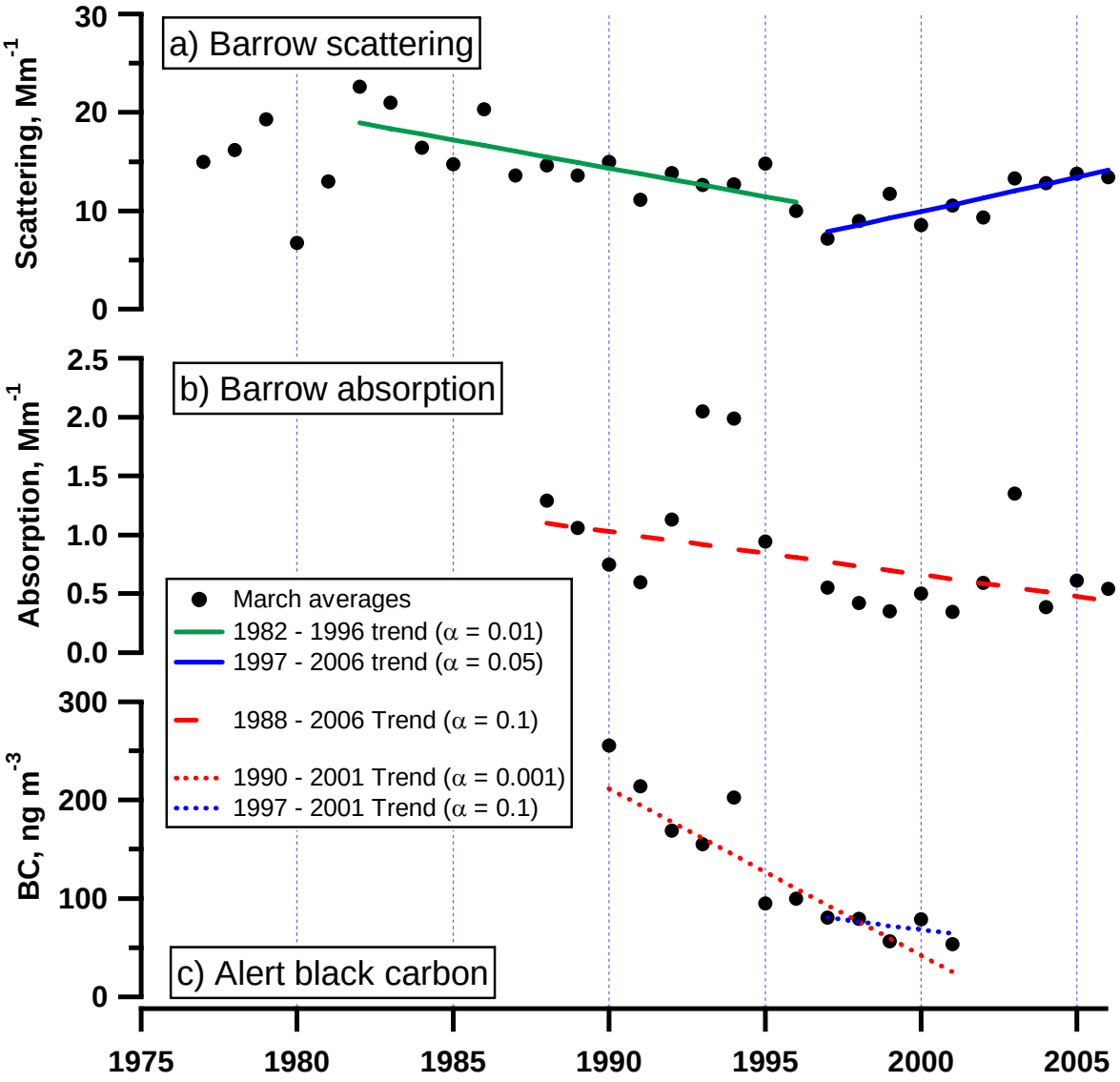

Figure 9. Monthly averaged concentrations for March of a) light scattering and b) light absorption (m^{-1}) at 550 nm for sub-10 micron aerosol at Barrow, and c) black carbon (ng m^{-3}) for Alert. Lines indicate the Sen's slope estimate for the periods indicated. The α value indicates the significance level of the trend. α = 0.001 indicates there is a 0.1% probability that the trend does not exist. Trend lines are not shown for α > 0.1. Data made available for Barrow by NOAA GMD and for Alert by the Canadian National Atmospheric Chemistry (NAtChem) Database and Analysis System.

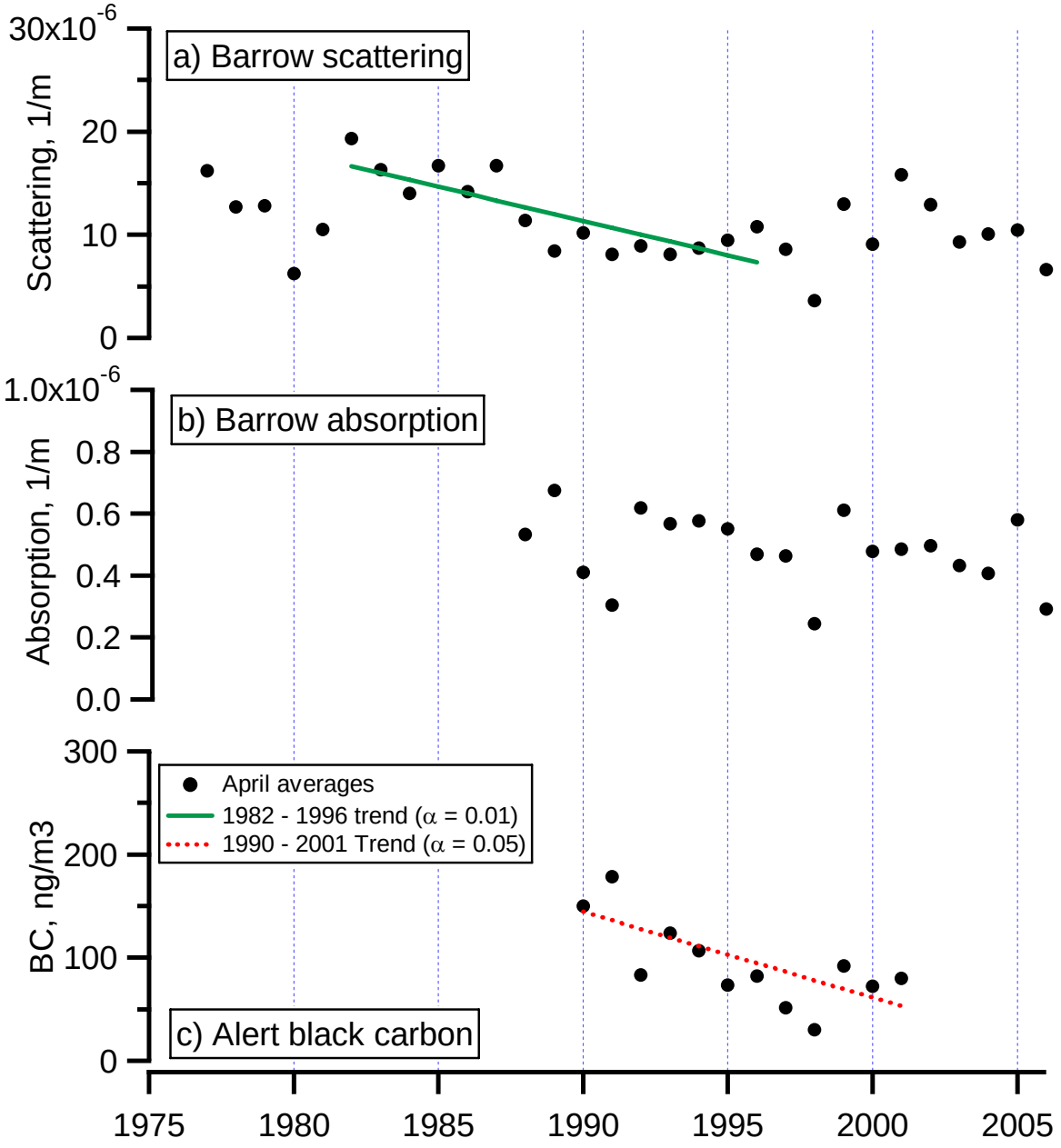

Figure 10. Monthly averaged concentrations for April of a) light scattering and b) light absorption (m^{-1}) at 550 nm for sub-10 micron aerosol at Barrow, and c) black carbon (ng m^{-3}) for Alert. Lines indicate the Sen's slope estimate for the periods indicated. The α value indicates the significance level of the trend. α = 0.001 indicates there is a 0.1% probability that the trend does not exist. Trend lines are not shown for α > 0.1. Data made available for Barrow by NOAA GMD and for Alert by the Canadian National Atmospheric Chemistry (NAtChem) Database and Analysis System.

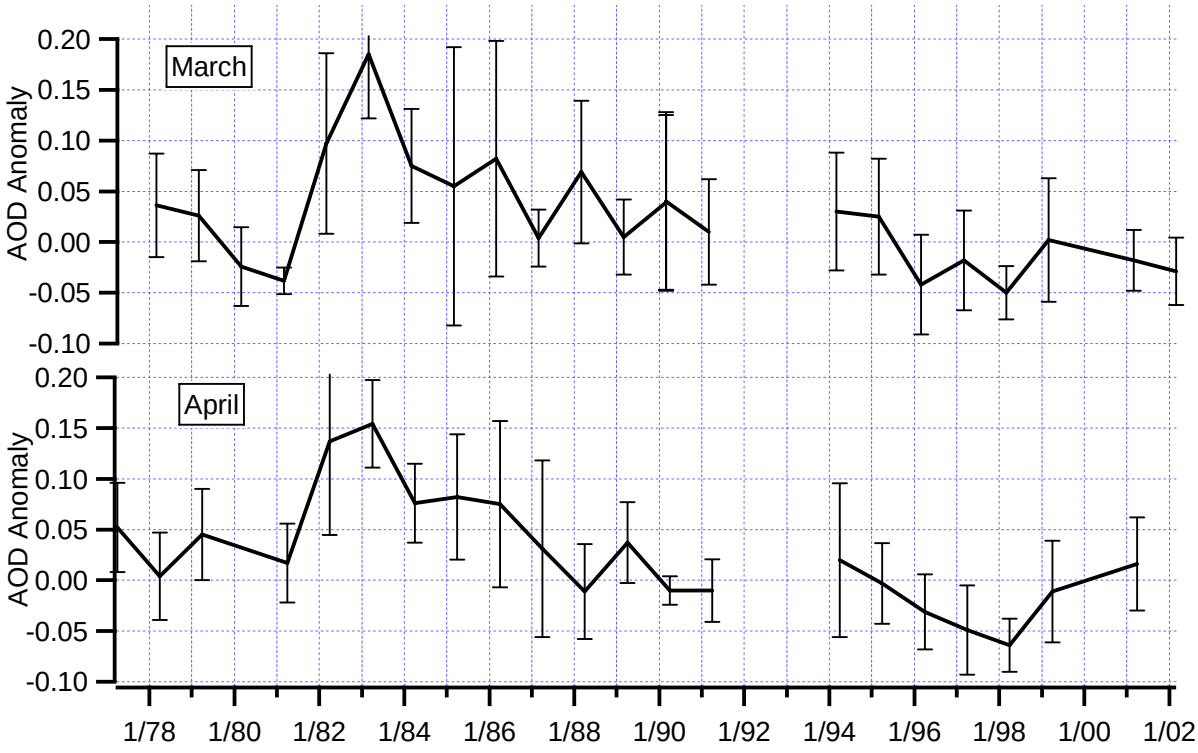

Figure 11. Monthly averaged AOD anomalies at Barrow, Alaska for March and April. The anomalies are relative to a base of non-volcanic years. Data from 1992 and 1993 were removed due to stratospheric aerosol influx from the Pinatubo eruption in 1991. Vertical lines represent the 1σ standard deviation of the monthly mean. Data made available by NOAA GMD.